Supporting Information

Layer-by-layer Assembled D/L-arginine-Calix[4]arene-Si-Surface for Macroscopic Enantio-selective Discrimination of (R)/(S)-ibuprofen

Xiong Li,[a†] Yingying Yang,[b†] Jiaxin Quan,[b†] Jin Zhang,[b] Ming Cheng,[b] Hewei Yan,[b] Siyun Zhang,[b] Lei Yang, [b] Zhiyan Lu*[c] and Haibing Li* [b]

Table of Contents

1. General methods

Chemicals and materials: All chemicals were A.R. grade and were purified by standard procedures. ^{1}H NMR and ^{13}C NMR were recorded on Varian Mercury VX600 instrument at ambient temperature with TMS as the internal standard. Mass Spectrometry (MS) were recorded on a Finnigan LCQ-Advantage instrument. The static water contact angle was measured at 25°C by means of an OCA 20 contact angle system (Dataphysics, Germany). The scanning electron microscope images were obtained at 25°C by means of a JSM-6700F HR-FESEM. All chemicals were A.R. grade and purified by standard procedures. Mill-Q water was used to prepare all solution.

UV-vis analysis: UV-vis analysis was carried out using UV-vis spectrometer in quart cell. D-arginine (1.0 mL, 1.0×10^{-3} mol L^{-1}) and (*R*)/(*S*)-ibuprofen as guests (100 μL, 1.0×10^{-2} mol L^{-1}) in H_2O was used. In the UV-vis titration experiment, 2.0 mL of D-arginine solution in H_2O and 0, 20, 40, 60, 80, 100, 120, 140, 160, 180, 200 μL of (*R*)/(*S*)-ibuprofen solution in H_2O were used, respectively.

X-ray photoelectron spectra experiment: X-ray photoelectron spectra (XPS) data were obtained with an ESCALab220i–XL electron spectrometer from VG Scientific using 300 W Al Kα radiation. Spectral calibration was determined by setting the main C1s component at 285 eV. The surface composition was estimated using the integrated peak areas.

The dynamic contact angle measurement: Contact angles were measured using an OCA 20 contact angle system (Dataphysics, Germany) at 25°C. The advancing and receding contact angle (ARCA) was measured, respectively, as adding and sucking off the liquid (3.0 μL) into and from the droplet on surface. The silicon surface was tilted to 42°, then 3.0 μL droplet was added onto it for observing the droplet sliding on surface. All images were recorded by OCA20.

Gaussian calculation: Computational calculations were carried out at the density functional theory b3lyp/6-31G (d) levels using Gaussian 03.

2. The procedure for the synthesis of diyne and dicarboxylic acid calix[4]arene

Scheme S1. Synthetic routes and procedures of diyne and dicarboxylic acid calix[4]arene **(C4AC)**

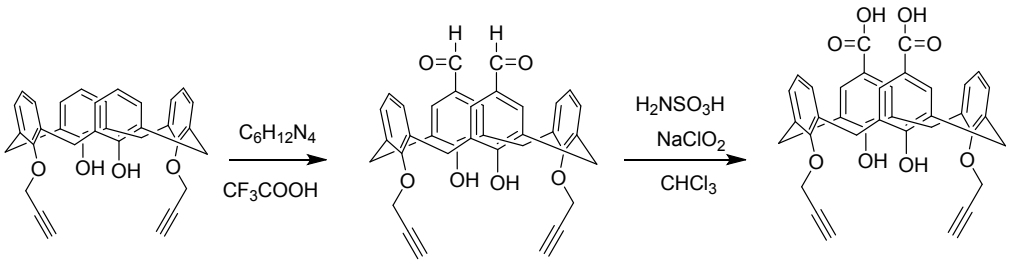

C4YA **C4AC**

Synthesis of diyne and dialdehyde calix[4]arene(C4YA). Diyne calix[4]arene (2.09 mmol) and hexamethylenetetramine (91.07 mmol) were added in trifluoroacetic acid (75 mL). The reaction mixture was refluxed until the starting materials had disappeared (TLC). Then, the mixture was quenched with ice cold water and extracted with chloroform. The organic layer was washed with water and dried with Na_2SO_4. The solvent was evaporated under reduced pressure, and the residue was purified by column chromatography as mentioned to yield the desired diyne and dialdehyde calix[4]arene (C4YA) product that the yield was 63.7%. ^{1}H NMR (400 MHz, $CDCl_3$) δ: 9.82 (s, 2H, CHO), 8.12 (s, 2H, ArOH), 7.65 (s, 4H, ArH), 6.92 (d, J = 7.6 Hz, 4H, ArH), 6.83 – 6.74 (m, J = 36.0 Hz, 2H, ArH), 4.83 (d, J = 2.4 Hz, 4H, $ArOCH_2$), 4.42 (d, J = 13.5 Hz, 4H, $ArCH_2Ar$), 3.54 (d, J = 13.5 Hz, 4H, $ArCH_2Ar$), 2.64 (t, J = 2.4 Hz, 2H, C≡CH). ^{13}C NMR (150 MHz, $CDCl_3$)δ: 190.87, 159.06, 151.10, 132.36, 130.90, 129.44, 128.66, 128.53, 126.12, 77.69, 63.69, 37.49, 31.60. ESI mass spectrum calculated for m/z=557.19, found m/z =557.286 ($M + H^+$).

Synthesis of diyne and dicarboxylic acid calix[4]arene (C4AC). In a 50 mL flask, diyne and dialdehyde calix[4]arene (100 mg) was dissolved in chloroform (10 mL) and acetone (30 mL) under an argon atmosphere. Sodium chlorite (64 mg) and sulfamic acid (70 mg) was solved in H_2O (1 mL), respectively. The sulfamic acid solution was first added in the flask, then added the sodium chlorite solution after 5min. The mixture was stirred for 12 h at ambient temperature until the solution appeared the faint yellow and the starting materials had disappeared (TLC). More diluted hydrochloric acid was added in the reactive solution and the yellow precipitate was separated out. The mixture filtered to get the precipitate and washed by dichloromethane. The precipitate was the product of diyne and dicarboxylic acid calix[4]arene that the yield is 83%. ^{1}H NMR (400 MHz, DMSO) δ: 12.43 (s, 2H, COOH), 8.23 (s, 2H, ArOH), 7.82 (s, 4H, ArH), 7.01 (d, J = 7.5 Hz, 4H, ArH), 6.81 (t, J = 7.5 Hz, 2H, ArH), 4.89 (s, 4H, $ArOCH_2$), 4.28 (d, J = 13.1 Hz, 4H, $ArCH_2Ar$), 3.74(s, 2H, ArOH), 3.59 (d, J = 13.2

Hz, 4H, $ArCH_2Ar$). ^{13}C NMR (150 MHz, $CDCl_3$) δ: 167.29, 156.85, 151.34, 133.25, 130.40, 129.20, 127.69, 125.85, 121.58, 79.95, 78.67, 63.73, 30.84. ESI mass spectrum calculated for m/z=987.422, found m/z= 588.67(M^+).

Scheme S2. Synthetic routes and procedures of 4-propargyloxy benzoic acid **(MC4AC)**

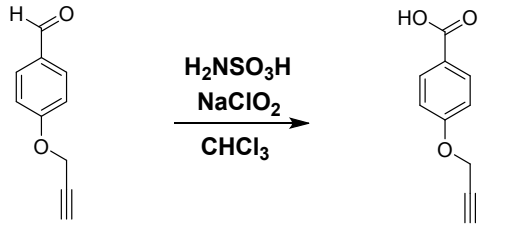

MC4AC

Synthesis of 4-propargyloxy benzoic acid (MC4AC). In a 50 mL flask, 4-(2-Propynyloxy) benzenecarbaldehyde (100 mg) was dissolved in chloroform (10 mL) and acetone (30 mL) under an argon atmosphere. Sodium chlorite (64 mg) and sulfamic acid (70 mg) was solved in H_2O (1 mL), respectively. The sulfamic acid solution was first added in the flask, then added the sodium chlorite solution after 5min. The mixture was stirred for 12h at ambient temperature until the solution appeared the faint yellow and the starting materials had disappeared (TLC). More diluted hydrochloric acid was added in the reactive solution and the yellow precipitate was separated out. The mixture filtered to get the precipitate and washed by dichloromethane. The precipitate was the product of 4-propargyloxy benzoic acid (MC4AC) that the yield is 91%. ^1H NMR (400 MHz, DMSO) δ: 12.67 (s, H, COOH), 7.90-7.93 (d, J =12.0 Hz, 2H, ArH), 7.06-7.09 (d, J = 7.5 Hz, 2H, ArH), 4.89-4.90 (s, 4H, $ArOCH_2$), 3.62(s, H, CCH). ^{13}C NMR (150 MHz, DMSO) δ: 167.36, 161.20, 131.73, 124.16, 115.12, 79.21, 79.11, 56.12. ESI mass spectrum calculated for m/z=176.02, found m/z= 176.26 (M^+). Anal. Calc. for $C_{10}H_8O_3$: C, 68.18; H, 4.57; O, 27.25. Found: C, 68.32; H, 4.63; O, 27.05.

3. The procedure for the C4AC and D/L-arginine modified on the surface

Scheme S3. The process of D/L-arginine assembled diyne and dicarboxylic acid calix[4]arene (C4AC) modified on the silicon surface.

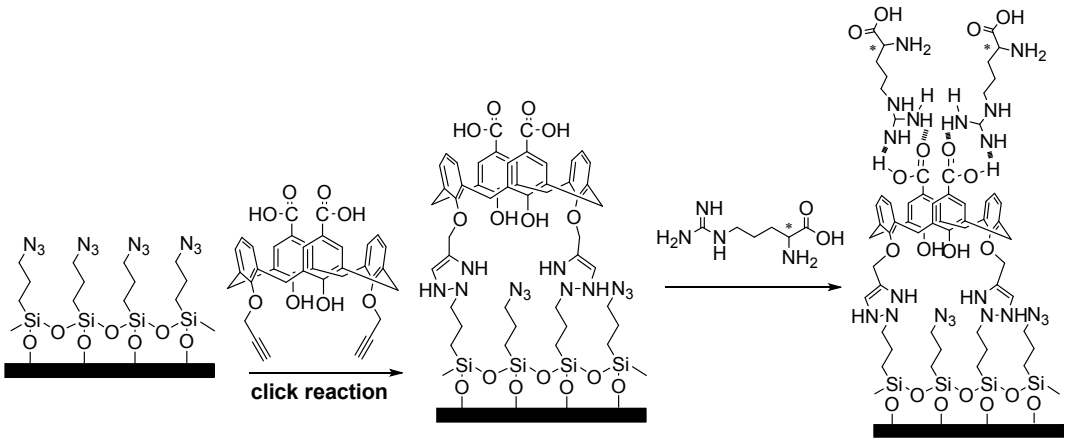

Fabrication of the micro–structure silicon surface. The silicon wafer was used directly as the smooth substrate. The structured silicon substrate was fabricated by the combination of the photolithography and inductively coupling plasma (ICP) deep etching technique. The photolithography and ICP technique were used to obtain the patterned silicon micropillar structure on silicon wafer. A rough surface introduced geometrical structures with patterned square pillars on a flat silicon wafer, 20 μm high, 4 μm long and with spacing of 6 μm between the silicon pillars.

Si–N_3 modified on the silicon surface. Silicon surfaces cut into 1 cm × 1 cm square pieces were soaked in chromosulfuric acid solution for 30 min and then rinsed with double distilled water and dried under a stream of N_2 gas. The cleaned wafers were immersed in aqueous NaOH (0.1 mol L^{-1}) for 6min and subsequently in HNO_3 (0.1 mol L^{-1}) for 12min to generate surface hydroxyl groups. After the silicon substrates had been washed with an excess of double distilled water and dried under a stream of N_2 flow, they were immersed in a refluxing solution of 5 wt% Si–N_3 in dry toluene (10 mL) at 110°C for 6h. Then it was washed with toluene and ethanol to remove the excess Si–N_3 and dried under a stream of N_2 gas.

The C4AC modified on the Si–N_3-silicon surface through the click reaction. The silicon substrate modified with Si-N_3 was immersed in **C4AC** solution (10^{-3} mol L^{-1} in CH_3CN). The mixture water of copper sulfate (10^{-6} mol L^{-1}) and sodium ascorbate (10^{-7} mol L^{-1}) were added into this solution, which was kept at 75°C for 8h. Then the silicon wafer was washed with CH_3CN and dried under a stream of N_2 gas.

D/L-arginine assembled on the C4AC modified silicon surface. C4AC modified silicon surface was under 50°C, 1.0 x 10^{-3} mol L^{-1} in the aqueous solution of D/L-arginine modified

4 h, respectively. Arginine is assembled on the C4AC modified silicon surface with secondary water flushing three times. Then, the functional silicon surface dried under a stream of N_2 gas.

Scheme S4. The process of D/L-arginine assembled 4-propargyloxy benzoic acid (MC4AC) modified on the silicon surface.

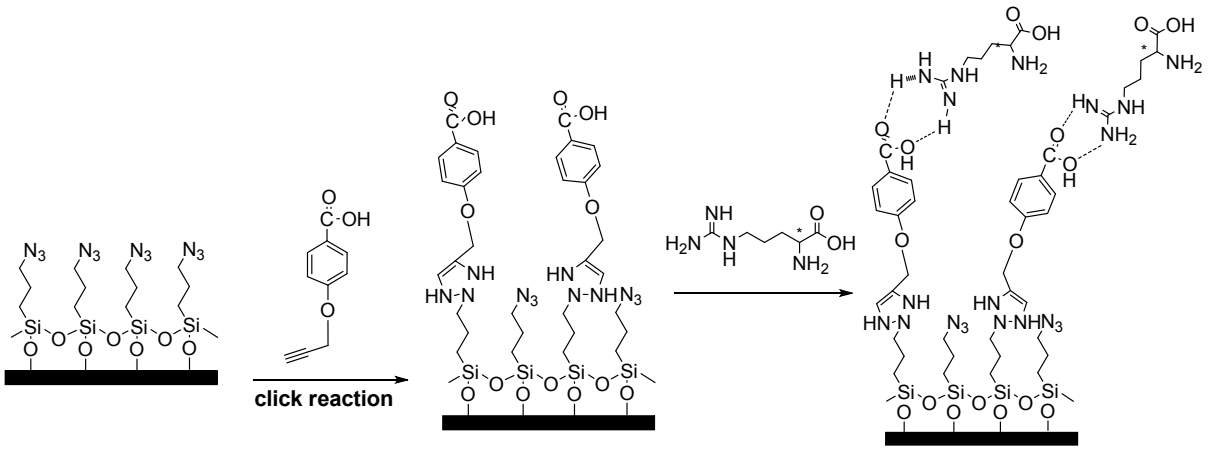

The MC4AC modified on the Si–N_3-silicon surface through the click reaction. The silicon substrate modified with Si-N_3 was immersed in **MC4AC** solution (10^{-3} mol L^{-1} in CH_3CN). The mixture water of copper sulfate (10^{-6} mol L^{-1}) and sodium ascorbate (10^{-7} mol L^{-1}) were added into this solution, which was kept at 75°C for 8h. Then the silicon wafer was washed with CH_3CN and dried under a stream of N_2 gas.

D/L-arginine assembled on the MC4AC modified silicon surface. MC4AC modified silicon surface was under 50°C, 1.0 x 10^{-3} mol L^{-1} in the aqueous solution of D/L-arginine modified 4h, respectively. Arginine is assembled on the MC4AC modified silicon surface with secondary water flushing three times. Then, the functional silicon surface dried under a stream of N_2 gas.

4. ^{1}H NMR , ^{13}C NMR and MS for the main compounds

^{1}H NMR (400 MHz, 293 K, $CDCl_3$) and ^{13}C NMR (150 MHz, 293 K, $CDCl_3$) spectra analysis of **C4YA**.

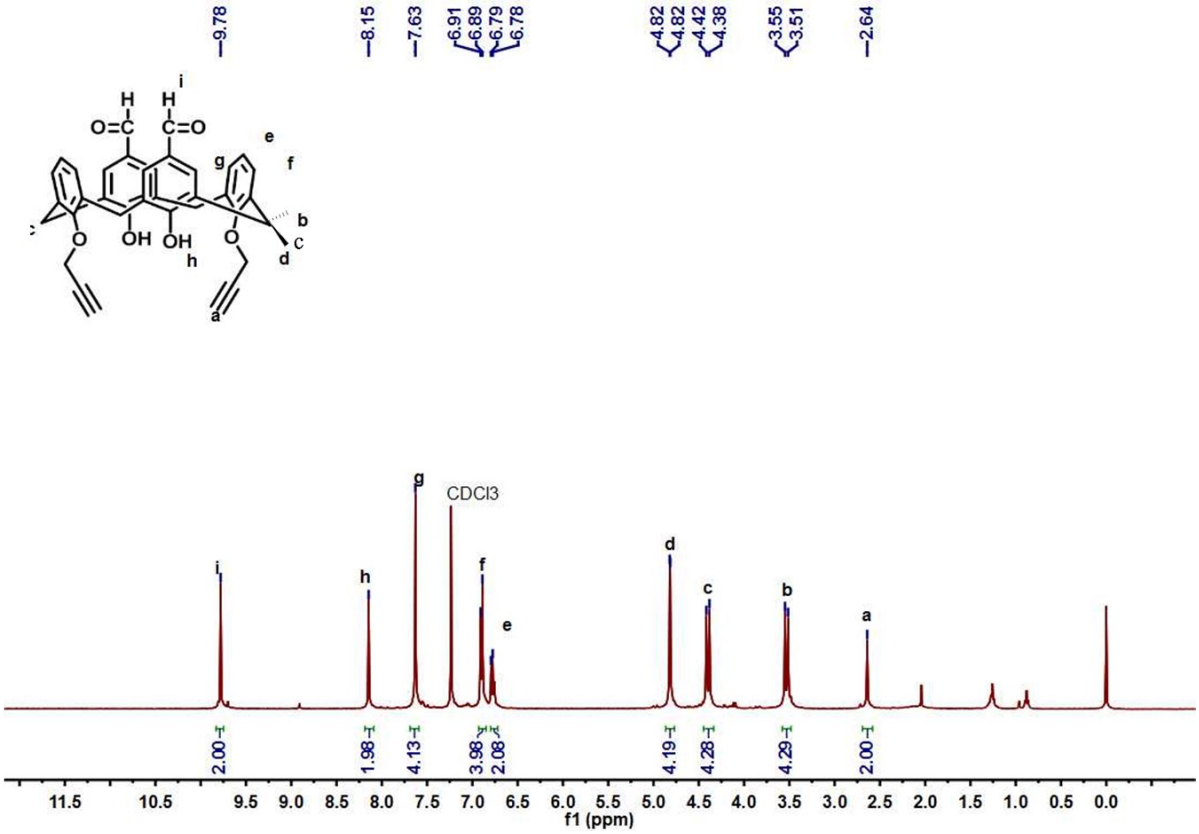

Figure S1. ^{1}H NMR (400 MHz, 293 K, $CDCl_3$) of **C4YA**.

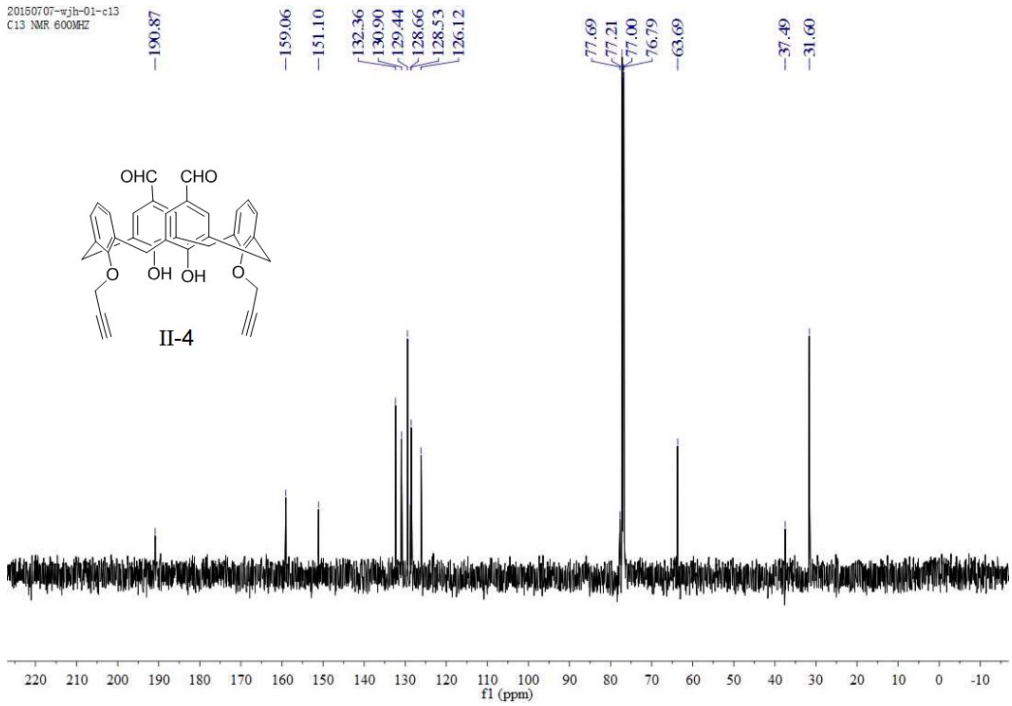

Figure S2. ^{13}C NMR (150 MHz, 293 K, $CDCl_3$) of **C4YA**.

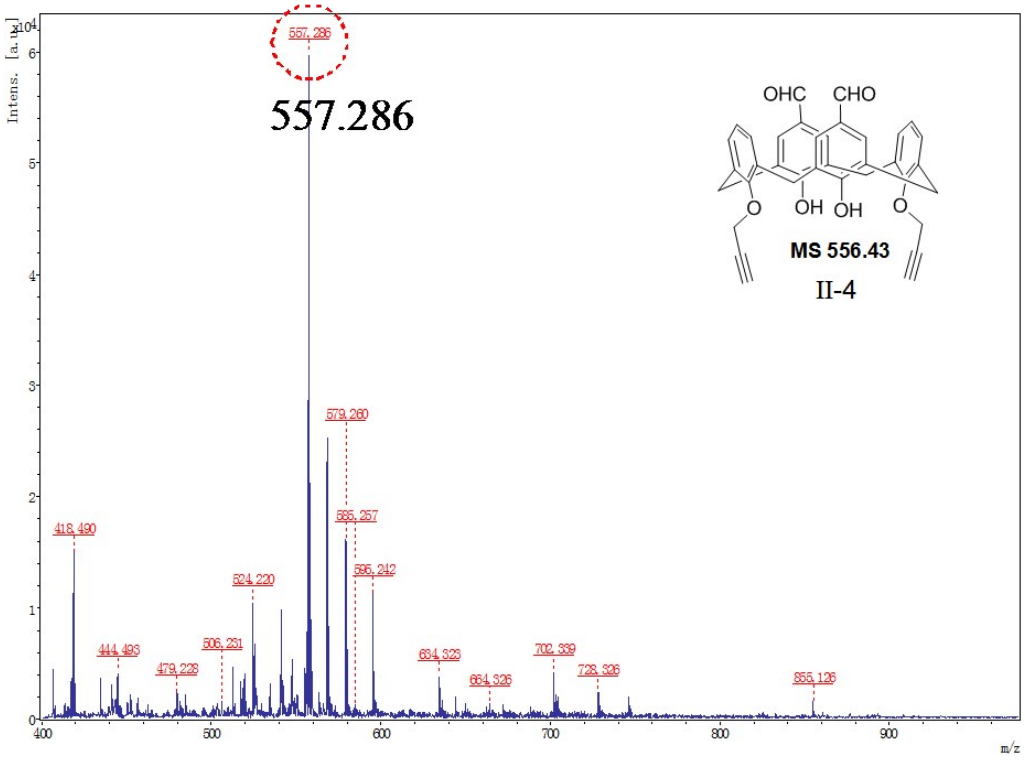

Figure S3. ESI mass spectrum of **C4YA**.

Spectra analysis of diyne and dicarboxylic acid calix[4]arene (C4AC) by ^{1}H NMR (400 MHz, 293 K, DMSO), ^{13}C NMR (150 MHz, 293 K, DMSO) and ESI mass spectrum.

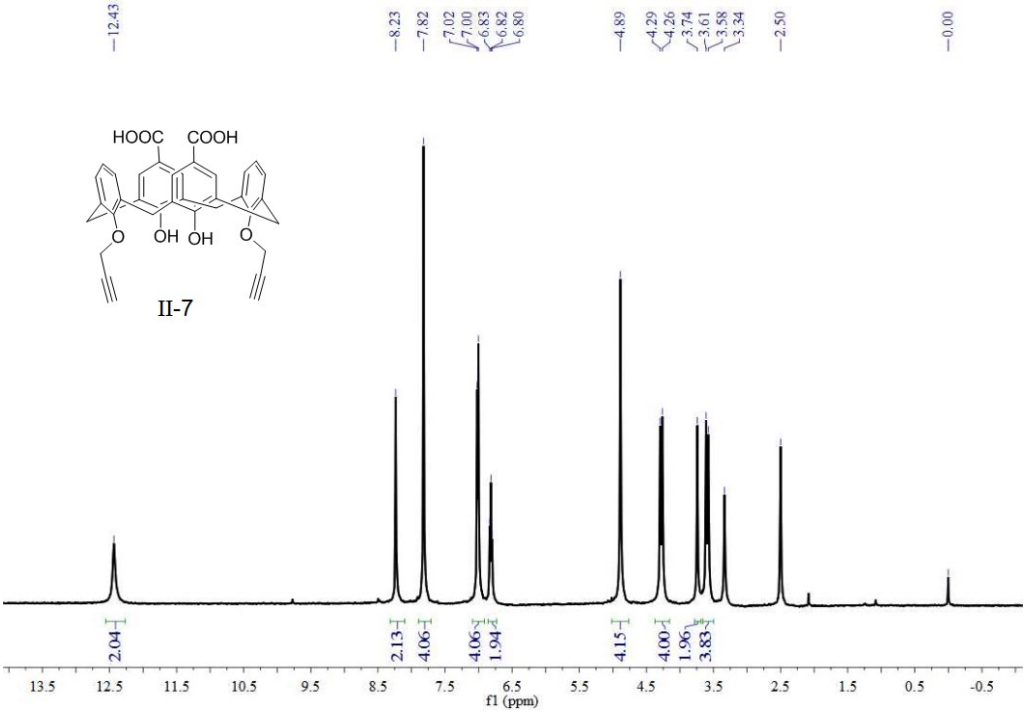

Figure S4. ^{1}H NMR (400 MHz, 293 K, DMSO) of diyne and dicarboxylic acid calix[4]arene.

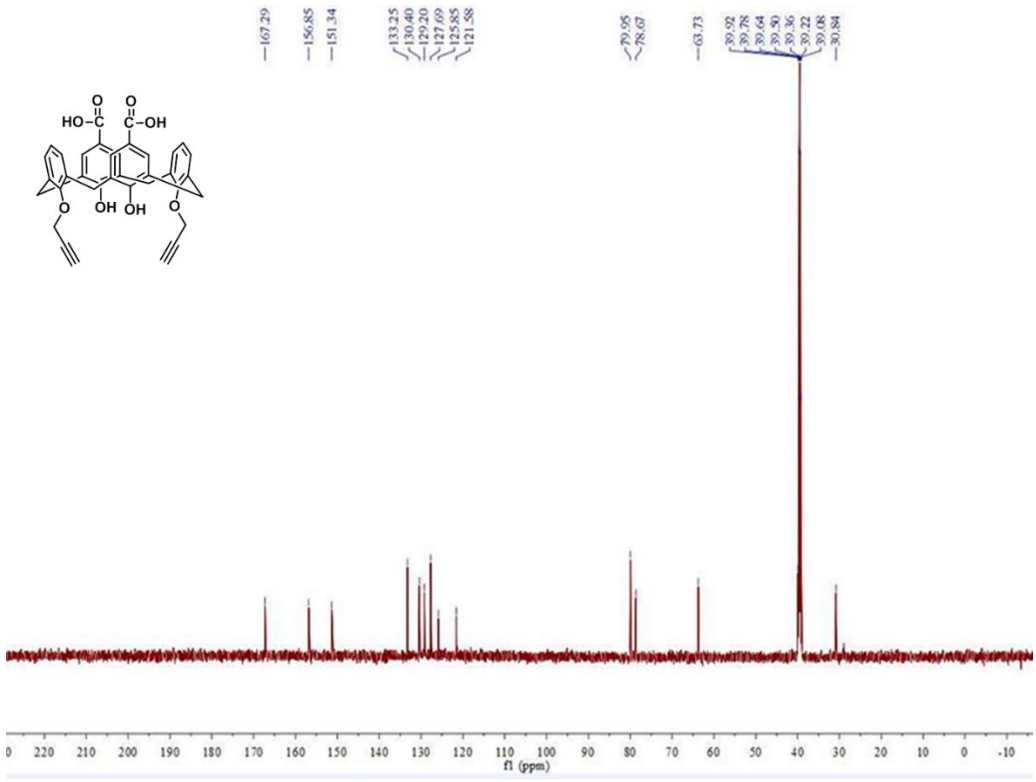

Figure S5. ^{13}C NMR (150 MHz, 293 K, DMSO) of diyne and dicarboxylic acid calix[4]arene.

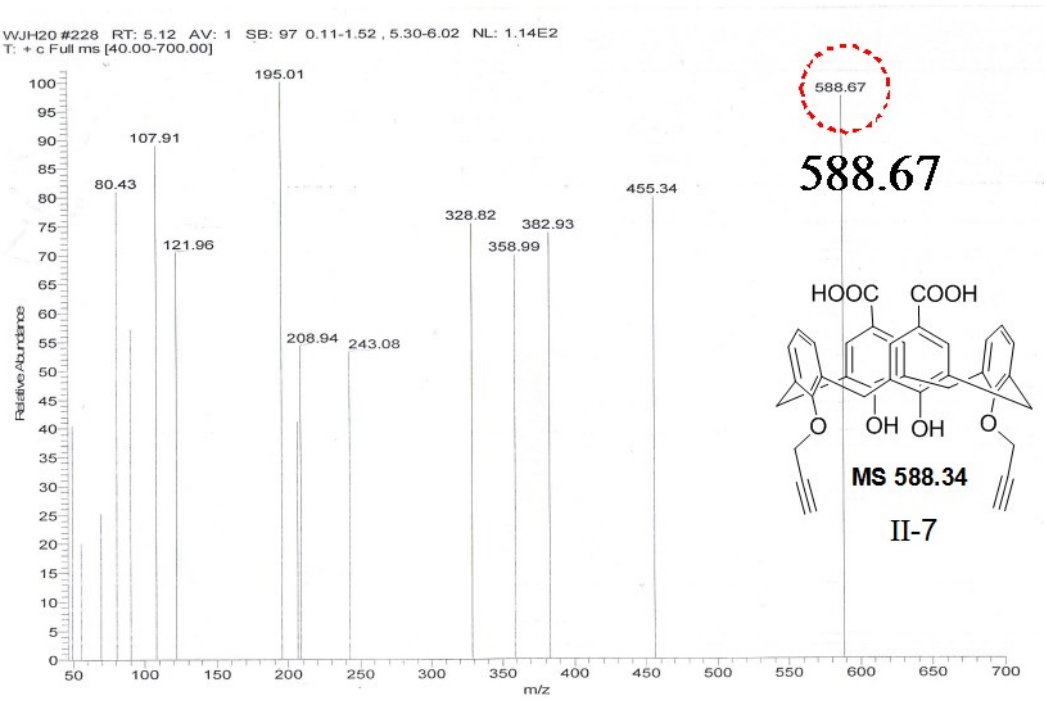

Figure S6. ESI mass spectrum of diyne and dicarboxylic acid calix[4]arene.

Spectra analysis of 4-propargyloxy benzoic acid (MC4AC) by ^{1}H NMR (400 MHz, 293 K, DMSO), ^{13}C NMR (150 MHz, 293 K, DMSO) and ESI mass spectrum.

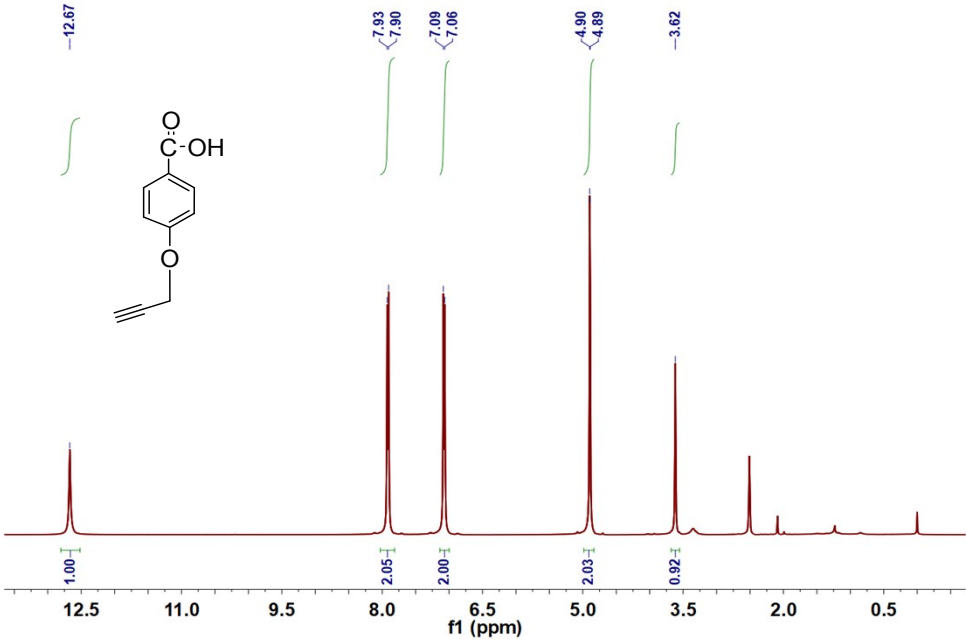

Figure S7. ^{1}H NMR (400 MHz, 293 K, DMSO) of 4-propargyloxy benzoic acid (MC4AC).

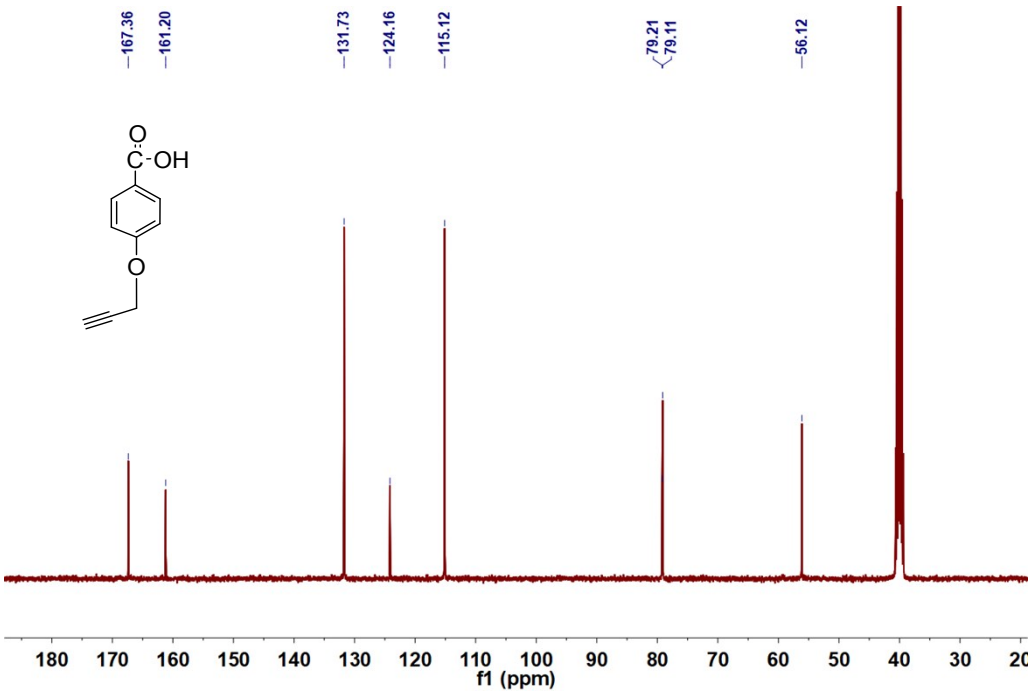

Figure S8. ^{13}C NMR (150 MHz, 293 K, DMSO) of 4-propargyloxy benzoic acid (MC4AC).

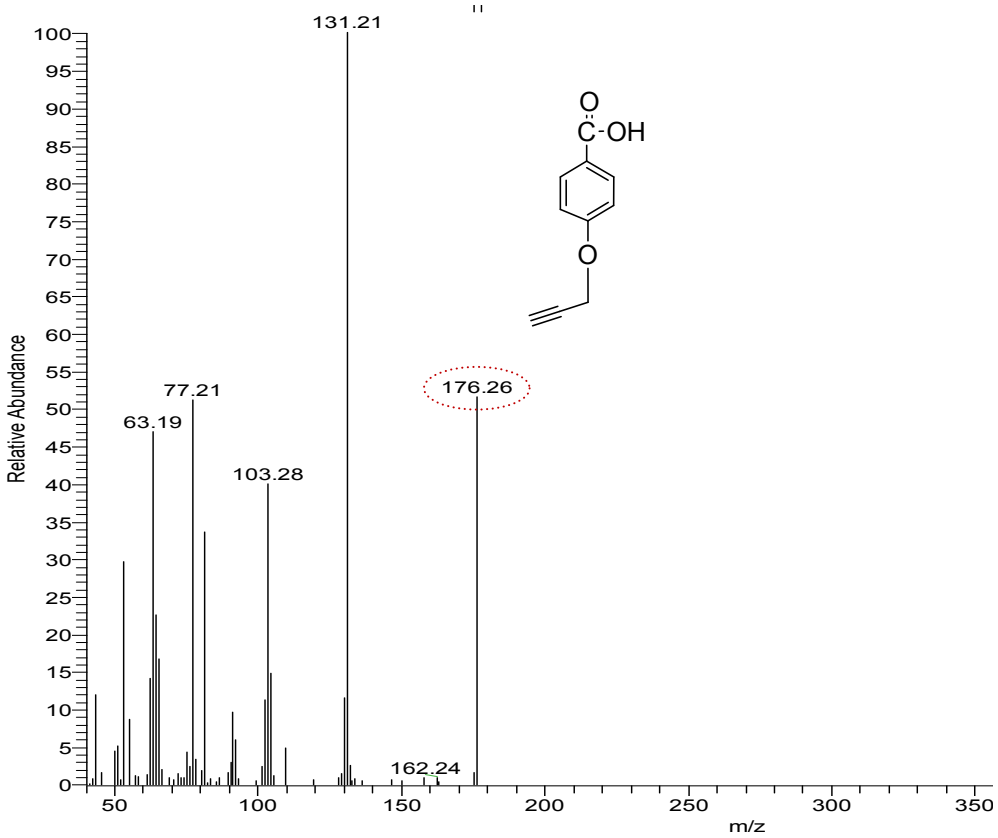

Figure S9. ESI mass spectrum of 4-propargyloxy benzoic acid (MC4AC).

5. *[1]H NMR characterization between Host and Guest*

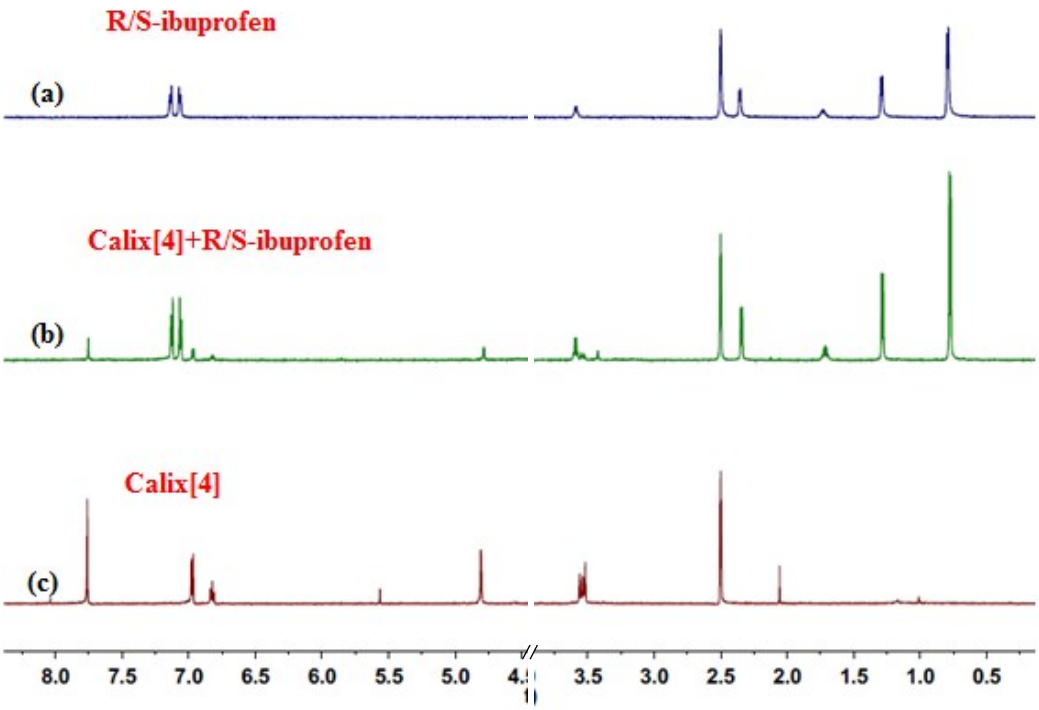

Figure S10. [1]H NMR (600MHz, 293K, DMSO), (a) (*R*)/(*S*)-ibuprofen; (b) C4AC and (*R*)/(*S*)-ibuprofen; (c) C4AC. As shown in figure, there are not the change of chemical shift which illustrate the C4AC and (*R*)/(*S*)-ibuprofen don't have the interaction.

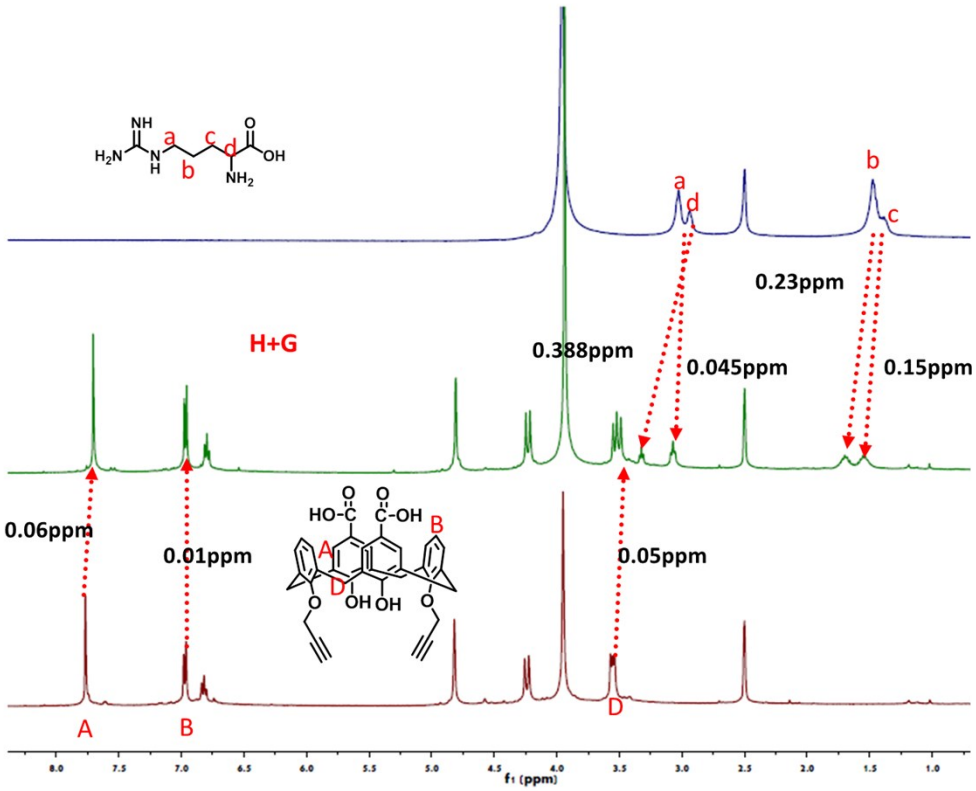

Figure S11. ^{1}H NMR (600MHz, 293K, DMSO), (a) D-arginine; (b) C4AC and D-arginine; (c) C4AC. There is the bigger change of chemical shift between the C4AC and D-arginine. It illustrates the C4AC and D-arginine is stable complex through the interaction of guanidine and carboxyl.

6. *UV-Vis and CD characterization for the D-arginine and (R)/(S)-ibuprofen*

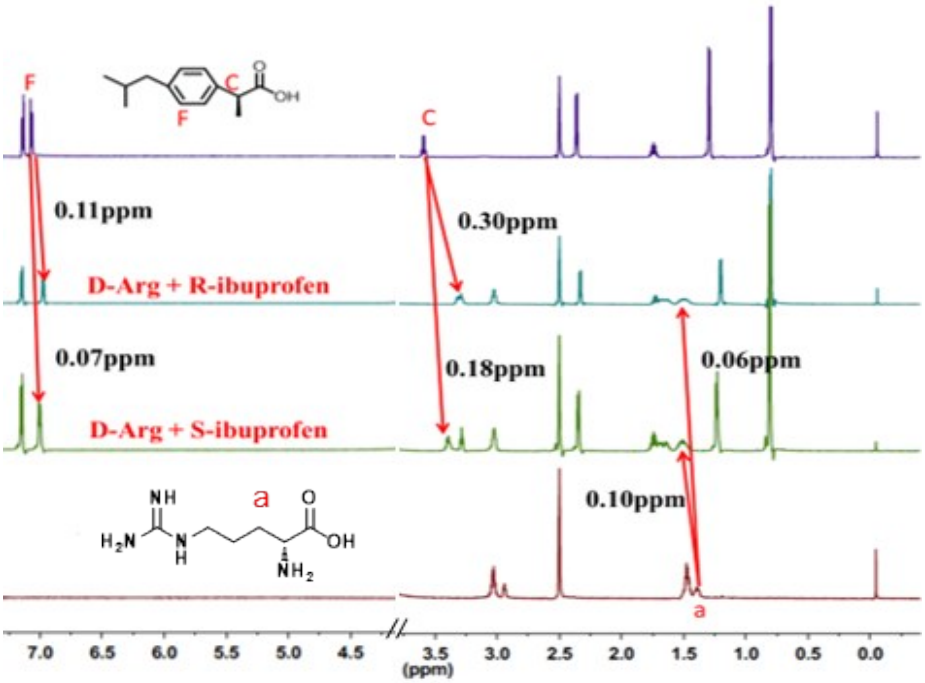

Figure S12. Partial ^{1}H NMR spectrum of the C4AC and (*R*)/(*S*)-ibuprofen illustrated the chemical shift change (6 mmol mL^{-1}, DMSO).

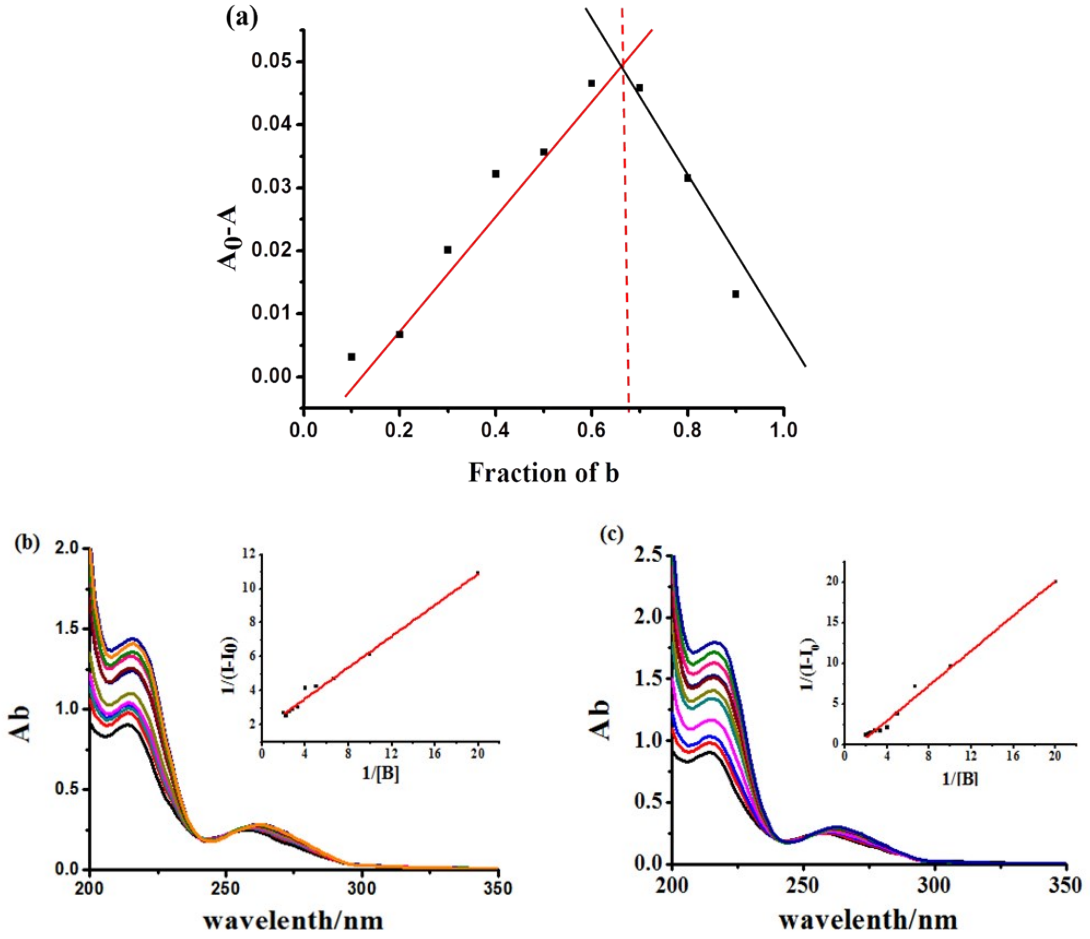

Figure S13. (a)The associated Job curve, and fitted according to a 1:2 binding stoichiometry, between (*R*)/(*S*)-ibuprofen and D-arginine. (b) The UV-vis titration of the D-arginine (10^{-3} mol L^{-1}, 2 mL) with (*S*)-ibuprofen(10^{-2} mol L^{-1}, 20, 40, 60, 80, 100, 120, 140, 160, 180 and 200 μL). (c) The UV-vis titration of the D-arginine (10^{-3} mol L^{-1}, 2 mL) with (*R*)-ibuprofen (10^{-2} mol L^{-1}, 20, 40, 60, 80, 100, 120, 140, 160, 180 and 200 μL). It was found that the ultraviolet absorption intensity of the mixed solution gradually increased with the increase of the concentration of (*R*)/(*S*)-ibuprofen. The signal enhancement degree of the absorption peak after the addition of (*R*)-ibuprofen was significantly greater than (*S*)-ibuprofen. The complex constant of D-Arg-C4AC and (*R*)-ibuprofen (K_R) was 6.85×10^3 M^{-1}. The complex constant of D-Arg-C4AC and (*S*)-ibuprofen (K_S) was 8.54×10^2 M^{-1}. In conclusion, D-Arg-C4AC and (*R*)-ibuprofen have a stronger force than (*S*)-ibuprofen.

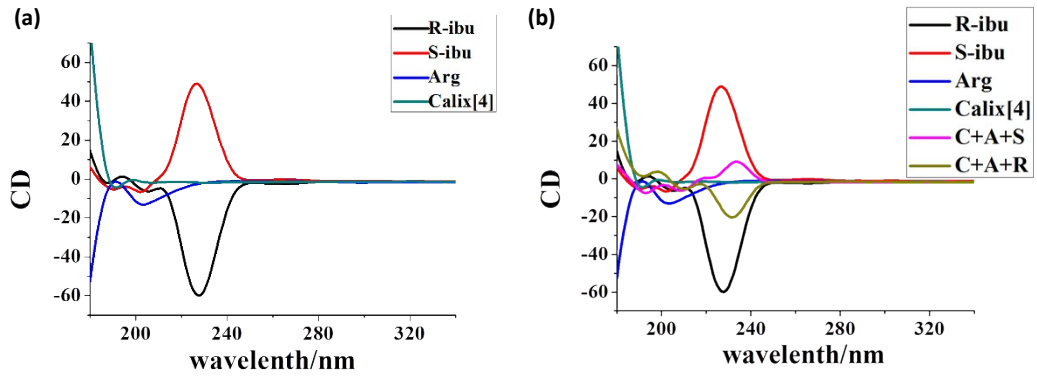

Figure S14. (a) Circular dichroism spectrum (CD) characterizes the C4AC, D-arginine and (*R*)/(*S*)-ibuprofen with the concentration of 10^{-3} mol L^{-1} in aqueous solution (2 mL); (b) The mixture of D-arginine assembled C4AC with (*R*)-ibuprofen and (*S*)-ibuprofen characterized by CD which the signal of (*R*)-ibuprofen is stronger than (*S*)-ibuprofen. This result illustrates the (*R*)-ibuprofen have the stronger interaction with D-arginine assembled C4AC.

7. XPS characterization of the Si-N_3 and C4AC modified surface

Element relative content of the Si-N_3 modified surface is distinct with the acetylene and dicarboxylic acid calix[4]arene (**C4AC**) modified surface. Just as the result of XPS in Table 1, after azide silane was modified on the silicon surface, the relative element content of carbon is 30.57%, nitrogen is 5.70% and oxygen is 36.01%, respectively. While the **C4AC** modified on the silicon surface, the relative element content of carbon is 43.50%, nitrogen is 3.43% and oxygen is 46.17%, respectively. By comparing the relative content of elements, we had found that the relative element content of nitrogen is reduced after **C4AC** modified, and the relative element content of carbon and oxygen is increased. The distinction between N_3-modified surface and **C4AC**-modified surface illustrated the **C4AC** modified successfully on the silicon surface.

Table S5 Content element

Name N_3-	Star BE	Peak BE	End BE	Atomi c%
C1s	290.32	284.92	282.33	30.57
O1s	535.06	535.73	527.67	36.01
N1s	406.87	400.22	395.92	5.70
Si2p	105.79	105.21	94.26	27.72

Name C4AC	Star BE	Peak BE	End BE	Atomi c%
C1s	292.15	284.53	282.60	43.50
O1s	534.98	548.72	527.79	46.17
N1s	406.28	399.87	395.76	3.43
Si2p	105.63	104.66	94.13	6.90

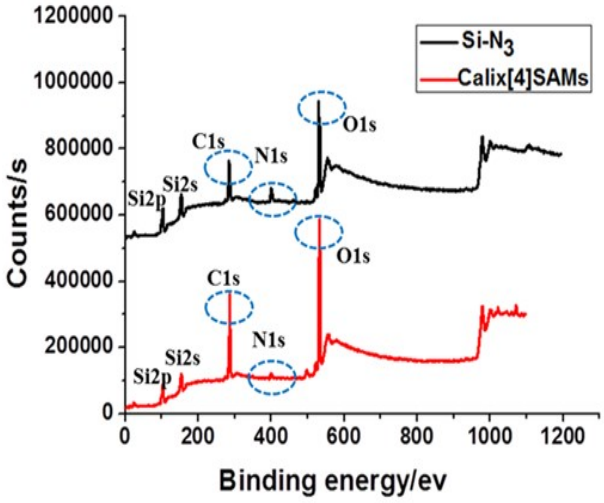

Figure S15. The element relative content observed in XPS is different before and after **C4AC** modified on the surface.

8. Contact angle characterization by the L-arginine assembled C4AC modified surface

The method of rolling contact angle on the inclined surface

Will be a big enough volume of droplet in the surface of the sample under test, the sample surface tilted toward one side slowly, continuously. At first the droplet doesn't move, and the liquid by the direction ahead after the transfer. It makes the front of contact angle increasing, while the rear narrowing. When inclined to a certain angle, droplet starts sliding. In sliding on the eve of rake angle of the droplet is advancing angle, other angle is back angle.

The dynamic and inclined contact angle of (*R*)/(*S*)-ibuprofen droplets on the D/L-arginine assembled C4AC modified surface

By dropping the object droplets of (*R*)/(*S*)-ibuprofen on the inclined D/L-arg-C4AC surface, the static contact angle did not have a clear distinction. We did research the properties of drop objects directly onto the L-arg-C4AC surface and then found that the contact angle hysteresis was 62.3±2.0° when added (*S*)-ibuprofen, while the contact angle hysteresis was 46.1±2.3° when added R-ibuprofen. It is mainly because of L-arg-C4AC surface have interactions with (*S*)-ibuprofen molecular which changed the chemical composition of the surface and increased the contact angle hysteresis value. The chiral matching force of (*R*)-ibuprofen with L-arg-C4AC was not stronger than (*S*)-ibuprofen, the contact angle hysteresis was smaller. The silicon surface modified with D/L-arg-C4AC exist the interaction with (*R*)/(*S*)-ibuprofen so that the contact angle hysteresis was increased. The contact angle hysteresis directly affects the degree of droplets rolled on the surface. By the theoretical formula $sin\alpha=\omega\gamma LA(cos\theta_{rec}-cos\theta_{adv})$/mg, while α was the roll angle, m was the drops quality, γLA was the surface tension of the droplet, ω was the width of the droplet, θ_{rec} was the recession angle, θ_{adv} was the advance angle.

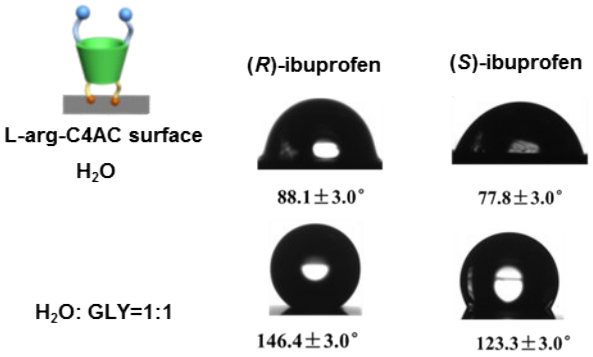

Figure S16. Static contact angle of (*R*)/(*S*)-ibuprofen aqueous droplets (2.0 μL, 10^{-3} mol L^{-1}) on L-arg-C4AC-surface were 88.1±2.9° and 77.8±2.3° which don't have the difference. The solvents of H_2O and glycerol (1:1) were selected to increase the hydrophobic property. Static contact angle of the mixed solvents of (*R*)/(*S*)-ibuprofen droplets (2.0 μL, 10^{-3} mol L^{-1}) on L-arg-C4AC surface were 146.3±3.2° and 123.5±2.8° which don't have the obvious distinction.

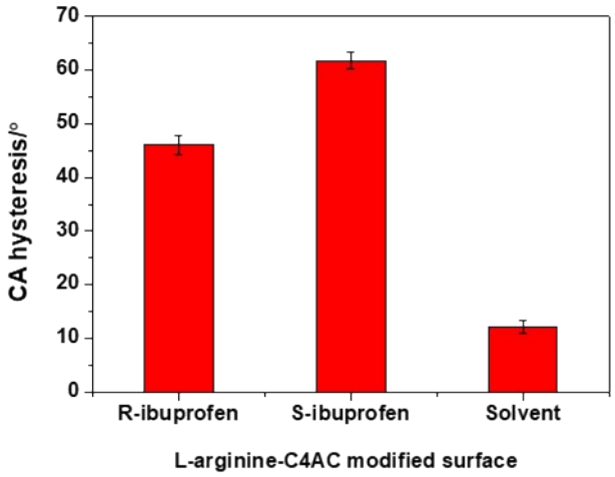

Figure S17. The column of contact angle hysteresis was tested through the drop (*R*)/(*S*)-ibuprofen (3.0 μL, 10^{-3} mol L^{-1}) on D-arg-C4AC surface. There were 46.1±2.3° and 62.3±2.0°, respectively.

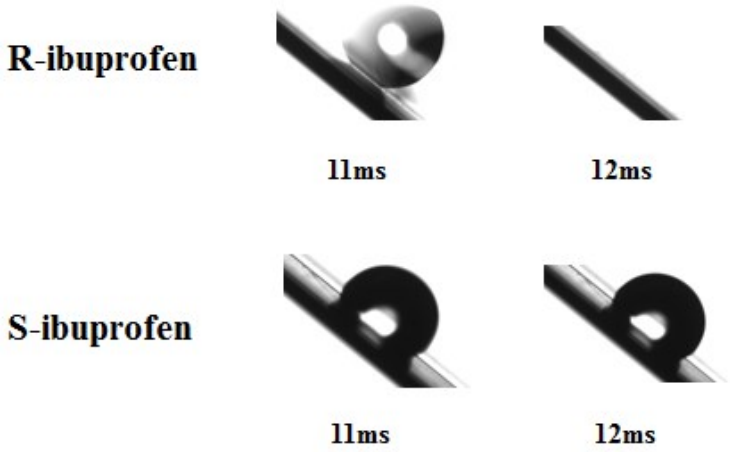

Figure S18. The chiral recognition of (*R*)/(*S*)-ibuprofen droplets on the inclined L-arg-C4AC-surface with 42° title angle, respectively. This presented the chiral selective adhesion to macroscopic droplet of (*S*)-ibuprofen by L-arg-C4AC surface with 42° title angle.

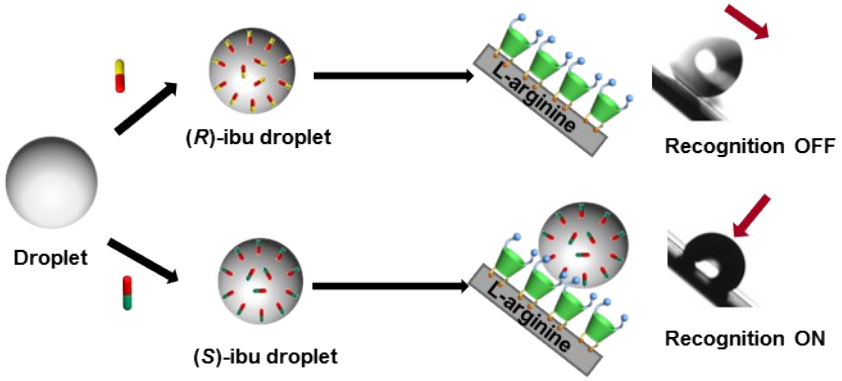

Figure S19. The specific recognition of macroscopic chiral recognition of (*S*)-ibuprofen droplet on the L-arg-C4AC-surface.

9. The calculation of the equilibrium adsorption constant

The difference fluorescence intensity of (*R*)-ibuprofen and (*S*)-ibuprofen at different concentrations(0.025, 0.05, 0.1, 0.25, 0.5, 0.75, 0.1mmol L^{-1}). We soaked D-arg-C4AC surface in ibuprofen for 3h, and measured the fluorescence intensity (excitation wavelength was 290nm) before (I_0) and after (I_i) immersion.The fluorescence intensity before immersion was subtracted from the fluorescence concentration after immersion to get the figure S20. The software used for fitting is Origin 2018.

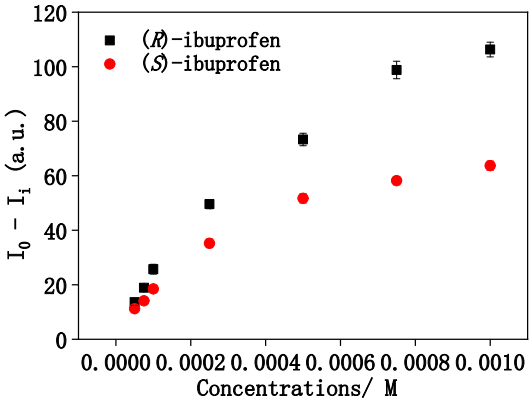

Figure S20. The difference in fluorescence intensity of (*R*)-ibuprofen and (*S*)-ibuprofen at different concentrations.

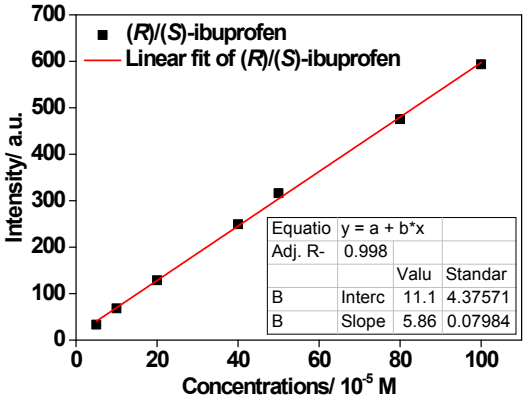

Figure S21. The working curve of (*R*)/(*S*)-ibuprofen's fluorescence emission spectrum.

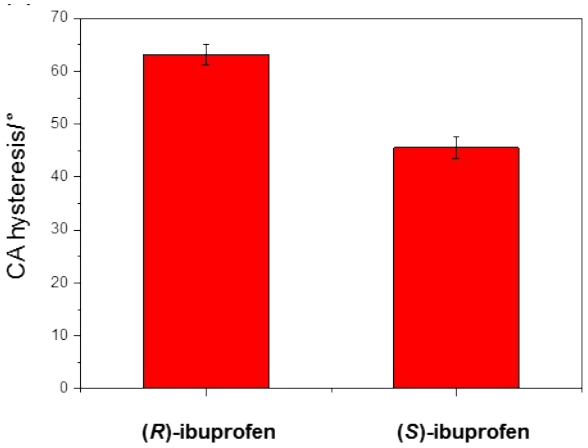

Figure S22. The column of contact angle hysteresis were tested through the drop (*R*)/(*S*)-ibuprofen (3.0 μL, 10^{-3} mol L^{-1}) on D-arginine assembled C4AC-surface. There were 63.1±1.9° and 45.6±2.1°, respectively.

10. The crystal structure of diyne and dialdehyde calix[4]arene (C4YA) and (b) dimer of diyne and dialdehyde calix[4]arene

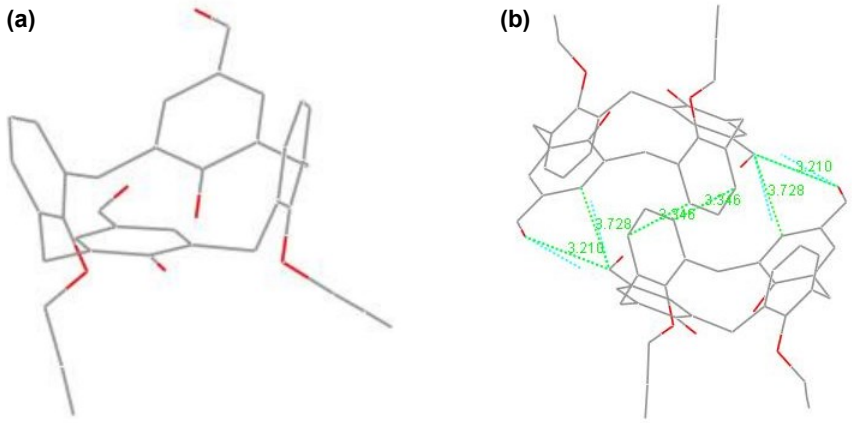

Figure S23. (a) The crystal structure of diyne and dialdehyde calix[4]arene (C4YA) and (b) dimer of diyne and dialdehyde calix[4]arene (C4YA).

Table S2. The length of bond for the crystal structure of diyne and dialdehyde calix[4]arene

Bonds	Bond Lengths (Å)	Bonds	Bond Lengths (Å)
C(1)-C(2)	1.388(5)	C(19)-C(20)	1.369(5)
C(1)-C(6)	1.394(5)	C(19)-H(19)	0.9300
C(1)-O(1)	1.395(4)	C(20)-H(20)	0.9300
C(2)-C(3)	1.390(5)	C(21)-C(22)	1.528(5)
C(2)-C(28)	1.509(5)	C(21)-H(21A)	0.9700
C(3)-C(4)	1.384(6)	C(21)-H(21B)	0.9700
C(3)-H(3)	0.9300	C(22)-C(27)	1.377(5)
C(4)-C(5)	1.371(6)	C(22)-C(23)	1.404(5)
C(4)-H(4)	0.9300	C(23)-O(4)	1.354(4)
C(5)-C(6)	1.378(5)	C(23)-C(24)	1.402(5)
C(5)-H(5)	0.9300	C(24)-C(25)	1.371(5)
C(6)-C(7)	1.517(5)	C(24)-C(28)	1.511(5)
C(7)-C(8)	1.513(5)	C(25)-C(26)	1.386(5)
C(7)-H(7A)	0.9700	C(25)-H(25)	0.9300
C(7)-H(7B)	0.9700	C(26)-C(27)	1.389(5)
C(8)-C(13)	1.376(5)	C(26)-C(36)	1.475(5)
C(8)-C(9)	1.406(5)	C(27)-H(27)	0.9300
C(9)-O(2)	1.353(4)	C(28)-H(28A)	0.9700
C(9)-C(10)	1.400(5)	C(28)-H(28B)	0.9700

C(10)-C(11)	1.369(5)	C(29)-O(1)	1.429(4)
C(10)-C(14)	1.513(5)	C(29)-C(30)	1.454(6)
C(11)-C(12)	1.394(5)	C(29)-H(29A)	0.9700
C(11)-H(11)	0.9300	C(29)-H(29B)	0.9700
C(12)-C(13)	1.385(5)	C(30)-C(31)	1.166(6)
C(12)-C(32)	1.464(5)	C(31)-H(31)	0.9300
C(13)-H(13)	0.9300	C(32)-O(5)	1.217(5)
C(14)-C(15)	1.513(5)	C(32)-H(32)	0.9300
C(14)-H(14A)	0.9700	C(33)-C(34)	1.426(6)
C(14)-H(14B)	0.9700	C(33)-O(3)	1.436(4)
C(15)-C(16)	1.389(5)	C(33)-H(33)	0.9300
C(15)-C(20)	1.399(5)	C(34)-C(35)	1.175(6)
C(16)-C(17)	1.390(5)	C(35)-H(35)	0.9300
C(16)-O(3)	1.403(4)	C(36)-O(6)	1.211(5)
C(17)-C(18)	1.385(5)	C(36)-H(36)	0.9300
C(17)-C(21)	1.517(5)	O(2)-H(2)	0.8200
C(18)-C(19)	1.386(5)	O(4)-H(4A)	0.8200

Table S3. The angle of bond crystal structure of diyne and dialdehyde calix[4]arene

Angles	(°)	Angles	(°)
C(2)-C(1)-C(6)	122.4(3)	C(20)-C(19)-C(18)	120.2(3)
C(2)-C(1)-O(1)	118.0(3)	C(20)-C(19)-H(19)	119.9
C(6)-C(1)-O(1)	119.3(3)	C(18)-C(19)-H(19)	119.9
C(1)-C(2)-C(3)	117.8(3)	C(19)-C(20)-C(15)	121.5(3)
C(1)-C(2)-C(28)	122.0(3)	C(19)-C(20)-H(20)	119.2
C(3)-C(2)-C(28)	120.1(3)	C(15)-C(20)-H(20)	119.2
C(4)-C(3)-C(2)	120.4(4)	C(17)-C(21)-C(22)	113.5(3)
C(4)-C(3)-H(3)	119.8	C(17)-C(21)-H(21A)	108.9
C(2)-C(3)-H(3)	119.8	C(22)-C(21)-H(21A)	108.9
C(5)-C(4)-C(3)	120.2(4)	C(17)-C(21)-H(21B)	108.9
C(5)-C(4)-H(4)	119.9	C(22)-C(21)-H(21B)	108.9
C(3)-C(4)-H(4)	119.9	H(21A)-C(21)-H(21B)	107.7
C(4)-C(5)-C(6)	121.5(4)	C(27)-C(22)-C(23)	117.8(3)
C(4)-C(5)-H(5)	119.3	C(27)-C(22)-C(21)	120.9(3)
C(6)-C(5)-H(5)	119.3	C(23)-C(22)-C(21)	121.3(3)

C(5)-C(6)-C(1)	117.5(3)	O(4)-C(23)-C(24)	119.6(3)
C(5)-C(6)-C(7)	120.8(3)	O(4)-C(23)-C(22)	119.1(3)
C(1)-C(6)-C(7)	121.7(3)	C(24)-C(23)-C(22)	121.3(3)
C(8)-C(7)-C(6)	113.9(3)	C(25)-C(24)-C(23)	118.4(3)
C(8)-C(7)-H(7A)	108.8	C(25)-C(24)-C(28)	121.1(3)
C(6)-C(7)-H(7A)	108.8	C(23)-C(24)-C(28)	120.4(3)
C(8)-C(7)-H(7B)	108.8	C(24)-C(25)-C(26)	121.7(3)
C(6)-C(7)-H(7B)	108.8	C(24)-C(25)-H(25)	119.1
H(7A)-C(7)-H(7B)	107.7	C(26)-C(25)-H(25)	119.1
C(13)-C(8)-C(9)	117.9(3)	C(25)-C(26)-C(27)	118.7(3)
C(13)-C(8)-C(7)	120.7(3)	C(25)-C(26)-C(36)	121.0(3)
C(9)-C(8)-C(7)	121.3(3)	C(27)-C(26)-C(36)	120.3(3)
O(2)-C(9)-C(10)	118.8(3)	C(22)-C(27)-C(26)	121.9(3)
O(2)-C(9)-C(8)	119.3(3)	C(22)-C(27)-H(27)	119.0
C(10)-C(9)-C(8)	121.8(3)	C(26)-C(27)-H(27)	119.0
C(11)-C(10)-C(9)	117.5(3)	C(2)-C(28)-C(24)	113.1(3)
C(11)-C(10)-C(14)	120.9(3)	C(2)-C(28)-H(28A)	109.0
C(9)-C(10)-C(14)	121.4(3)	C(24)-C(28)-H(28A)	109.0
C(10)-C(11)-C(12)	122.4(3)	C(2)-C(28)-H(28B)	109.0
C(10)-C(11)-H(11)	118.8	C(24)-C(28)-H(28B)	109.0
C(12)-C(11)-H(11)	118.8	H(28A)-C(28)-H(28B)	107.8
C(13)-C(12)-C(11)	118.4(3)	O(1)-C(29)-C(30)	114.0(3)
C(13)-C(12)-C(32)	119.7(3)	O(1)-C(29)-H(29A)	108.8
C(11)-C(12)-C(32)	121.7(3)	C(30)-C(29)-H(29A)	108.8
C(8)-C(13)-C(12)	121.8(3)	O(1)-C(29)-H(29B)	108.8
C(8)-C(13)-H(13)	119.1	C(30)-C(29)-H(29B)	108.8
C(12)-C(13)-H(13)	119.1	H(29A)-C(29)-H(29B)	107.7
C(15)-C(14)-C(10)	114.9(3)	C(31)-C(30)-C(29)	176.3(4)
C(15)-C(14)-H(14A)	108.5	C(30)-C(31)-H(31)	180.0
C(10)-C(14)-H(14A)	108.5	O(5)-C(32)-C(12)	125.4(4)
C(15)-C(14)-H(14B)	108.5	O(5)-C(32)-H(32)	117.3
C(10)-C(14)-H(14B)	108.5	C(12)-C(32)-H(32)	117.3
H(14A)-C(14)-H(14B)	107.5	C(34)-C(33)-O(3)	110.4(3)
C(16)-C(15)-C(20)	116.2(3)	C(34)-C(33)-H(33)	124.8

C(16)-C(15)-C(14)	122.6(3)	O(3)-C(33)-H(33)	124.8
C(20)-C(15)-C(14)	121.1(3)	C(35)-C(34)-C(33)	176.8(4)
C(15)-C(16)-C(17)	123.8(3)	C(34)-C(35)-H(35)	180.0
C(15)-C(16)-O(3)	118.3(3)	O(6)-C(36)-C(26)	124.9(4)
C(17)-C(16)-O(3)	117.8(3)	O(6)-C(36)-H(36)	117.6
C(18)-C(17)-C(16)	117.1(3)	C(26)-C(36)-H(36)	117.6
C(18)-C(17)-C(21)	121.3(3)	C(1)-O(1)-C(29)	116.0(3)
C(16)-C(17)-C(21)	121.6(3)	C(9)-O(2)-H(2)	109.5
C(17)-C(18)-C(19)	120.9(3)	C(16)-O(3)-C(33)	110.9(2)
C(17)-C(18)-H(18)	119.6	C(23)-O(4)-H(4A)	109.5

11. Energy change of D-arginine with C4AC by the Gaussian simulation

Table S6. Energy change of D-arginine with C4AC

$\Delta E = E_{(Complex)} - E_{(D\text{-}arginine)} - E_{(C4AC)}$

Item	Energy （*kJ/mol*）
ΔE	**-227.76**

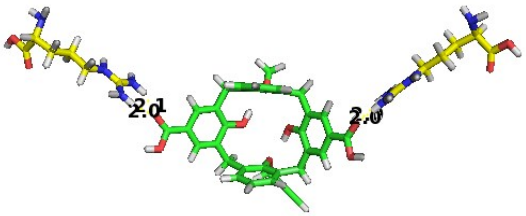

D-arginine assembled C4AC

The Gaussian simulation three-dimensional coordinates of C4AC and D-arginine interaction

N	18.2756	-0.0647	-3.8954
C	19.3091	-0.4442	-4.7424
N	19.1175	0.024	-6.0273
C	19.9867	-0.3863	-7.1104
C	19.5707	0.2992	-8.4082
H	21.155	-0.7545	-4.6247
C	20.4735	-0.1075	-9.5743
C	20.098	0.5077	-10.9244
C	20.3134	2.0111	-10.9413
O	19.7049	2.5939	-11.9714

N	20.2652	-1.1375	-4.2992
N	18.7226	0.1991	-11.279
O	20.9935	2.6202	-10.1825
H	18.4872	-0.2961	-2.9479
H	18.0039	0.8917	-3.9922
H	18.1538	0.0956	-6.2754
H	21.0023	-0.1017	-6.8589
H	19.9772	-1.4692	-7.2414
H	18.542	0.0445	-8.6419
H	19.612	1.3722	-8.2642
H	21.5016	0.1579	-9.3549
H	20.4487	-1.1892	-9.6927
H	20.8123	0.1335	-11.6643
H	19.9038	3.5251	-11.9462
H	20.1252	-1.3313	-3.3055
H	18.4787	0.6001	-12.1625
H	18.6021	-0.7926	-11.3508
H	7.4769	0.2637	-4.4335
N	4.5113	0.4978	-3.3632
C	5.6215	0.3934	-4.1915
N	5.2642	0.3424	-5.5244
C	6.2463	0.0656	-6.552
C	5.5908	0.0976	-7.9292
C	6.6027	-0.185	-9.0412
C	6.0162	-0.2101	-10.4545
C	5.5282	1.1608	-10.8897
O	4.7424	1.0971	-11.9617
N	6.7789	0.3484	-3.6918
N	4.9365	-1.1776	-10.5592
O	5.8037	2.191	-10.3678
H	4.7853	0.6634	-2.4179
H	3.8348	1.163	-3.6756
H	4.3775	-0.0901	-5.6729
H	7.018	0.8255	-6.4996

H	6.7303	-0.8988	-6.3921
H	4.7935	-0.6375	-7.971
H	5.1392	1.0712	-8.0776
H	7.3948	0.5548	-9.0158
H	7.0723	-1.1515	-8.8677
H	6.8369	-0.4264	-11.1454
H	4.4978	1.9852	-12.2045
H	6.879	1.071	-2.976
H	4.5551	-1.1947	-11.4839
H	5.2792	-2.0961	-10.354
C	12.7088	3.4338	2.6127
O	12.8997	2.3624	1.7196
C	12.7966	2.6227	0.3701
C	11.5417	2.7369	-0.2242
C	10.2391	2.501	0.5348
C	9.5056	1.2596	0.0554
C	8.4192	1.3448	-0.7899
C	7.7834	0.2003	-1.2604
C	6.6161	0.255	-2.1646
O	6.2371	1.4958	-2.4728
O	6.0416	-0.6957	-2.5989
C	8.2632	-1.0427	-0.8755
C	9.3437	-1.175	-0.0215
C	9.8534	-2.5595	0.355
C	11.1954	-2.8926	-0.2859
C	11.2629	-3.2204	-1.6323
C	12.4838	-3.4389	-2.2436
H	12.525	-3.6997	-3.2857
C	13.6536	-3.2909	-1.5217
C	13.6309	-2.9569	-0.1731
C	14.9373	-2.7087	0.572
C	15.6697	-1.4822	0.054
C	16.7469	-1.592	-0.7978
C	17.38	-0.4644	-1.3113

C	18.5311	-0.6537	-2.2178
O	18.9709	-1.7107	-2.5527
O	19.064	0.4887	-2.6535
C	16.9067	0.7917	-0.9626
C	15.8325	0.9497	-0.1021
C	15.3295	2.3433	0.2486
C	13.9745	2.6622	-0.3715
C	13.883	2.9312	-1.7302
C	12.6552	3.1338	-2.3306
H	12.5977	3.3517	-3.3818
C	11.4978	3.0184	-1.5834
C	15.2329	-0.201	0.4196
O	14.2251	-0.1676	1.2962
C	12.3867	-2.8093	0.4303
O	12.3046	-2.5007	1.7709
C	12.2593	-3.6096	2.6402
C	12.0132	-3.1398	4.0089
C	11.8064	-2.7866	5.1215
C	9.9479	-0.0076	0.4594
O	10.9601	-0.0091	1.3306
H	11.3024	-0.8676	1.5595
C	13.8594	4.3512	2.7091
C	14.764	5.111	2.8196
H	19.7911	0.2636	-3.2248
H	15.5709	5.7876	2.9143
H	13.9007	0.7013	1.5072
H	11.832	4.0025	2.3329
H	12.5271	2.9821	3.5774
H	10.4324	2.4042	1.5914
H	9.5898	3.3605	0.4002
H	8.0573	2.3102	-1.0895
H	5.4856	1.4286	-3.0529
H	7.7695	-1.9192	-1.2518
H	9.1192	-3.2868	0.0296

H	9.9129	-2.6519	1.4321
H	10.3552	-3.2921	-2.2054
H	14.6008	-3.4172	-2.0149
H	14.7434	-2.5903	1.6271
H	15.5829	-3.5727	0.452
H	17.1161	-2.5608	-1.0787
H	17.388	1.6639	-1.3628
H	16.0543	3.0642	-0.1108
H	15.2913	2.4705	1.3206
H	14.7815	2.9713	-2.3204
H	10.5426	3.1221	-2.0665
H	11.4708	-4.2901	2.339
H	13.1975	-4.1499	2.5984
H	11.6249	-2.4659	6.1124